

AGN Obscuring Tori Supported by Infrared Radiation Pressure

Julian H. Krolik

Department of Physics and Astronomy, Johns Hopkins University, Baltimore, MD 21218

ABSTRACT

Explicit 2-d axisymmetric solutions are found to the hydrostatic equilibrium, energy balance, and photon diffusion equations within obscuring tori around active galactic nuclei. These solutions demonstrate that infrared radiation pressure can support geometrically thick structures in AGN environments subject to certain constraints: the bolometric luminosity must be roughly $\sim 0.03\text{--}1\times$ the Eddington luminosity; and the Compton optical depth of matter in the equatorial plane should be ~ 1 , with a tolerance of about an order of magnitude up or down. Both of these constraints are at least roughly consistent with observations. In addition, angular momentum must be redistributed so that the fractional rotational support against gravity rises from the inner edge of the torus to the outer in a manner specific to the detailed shape of the gravitational potential. This model also predicts that the column densities observed in obscured AGN should range from $\sim 10^{22}$ to $\sim 10^{24}$ cm^{-2} .

Subject headings:

1. Background

Geometrically and optically thick belts of matter can be seen around many active galactic nuclei (Antonucci 1993). Although the evidence is best for nearby Seyfert galaxies (e.g., the direct detection by Jaffe et al. 2004 of the torus in NGC 1068), there is also strong indirect evidence that this picture applies to radio galaxies (Barthel 1989, di Serego Alighieri et al. 1994) and quasars (e.g., the spectropolarimetry presented in Zakamska et al. 2005). The ratio of observed numbers of obscured AGN to unobscured gives a measure of the fraction of opaque solid angle; it is generally ~ 1 (Hao et al. 2005). X-ray column densities to obscured nuclei range from $\sim 10^{22}$ cm^{-2} to in excess of 10^{24} cm^{-2} (Risaliti et al. 1999, Treister et al. 2004); applying a Galactic dust/gas ratio would imply a dust extinction $A_V \sim 10\text{--}10^3$ mag, easily ample for blocking the entire optical and ultraviolet continuum.

One of the principal puzzles about these tori is how they stand up against gravity. Orbital speeds in galactic potentials are generically ~ 100 km s^{-1} , and the nearby black hole

can only increase this characteristic speed. To stretch upward enough to block a significant fraction of solid angle requires a vertical velocity component that is a sizable fraction of the orbital speed; if the velocities are interpreted as thermal, temperatures of at least $\sim 10^5$ K are implied. If the gas is this hot, how can dust survive?

Numerous ideas have been proposed to answer this question, but none has proved entirely satisfactory. The first suggestion (made by Krolik & Begelman 1988 and elaborated by Beckert & Duschl 2004) was that the gas and dust are highly clumped, and the clumps have highly supersonic motions. To support these motions against the inevitable losses in cloud-cloud collisions, orbital shear energy can be randomized if magnetic fields make the clouds sufficiently elastic. The central problem with this scheme is that, although physically possible, the required magnetic field strengths are not terribly plausible. Another idea, almost as old, is that the gas and dust are always *locally* geometrically thin, but the plane in which they orbit varies as a function of radius (Sanders et al. 1989). Countering this suggestion are both the indirect evidence of well-formed “ionization cones” and polarized reflection regions collimated not far from the innermost part of the torus, and the direct evidence provided by detection of a geometrically thick structure right at the torus’s inner edge. Once again, one obtains the clearest view of all three sorts of data from NGC 1068 (Capetti et al. 1997, Kishimoto 1999, Jaffe et al. 2004). Still another suggestion was made by Königl & Kartje (1994), who argued that the large vertical motions required by geometrical thickness are best explained as arising in a magneto-centrifugal wind. The principal drawbacks to this idea are the unknown origin of the large-scale magnetic field and the large energy source needed to drive the wind. Still another idea is that magnetic fields alone support a static equilibrium (Lovelace et al. 1998). The last notional explanation to list is that the large optical/ultraviolet radiation flux of the AGN is converted to mid-infrared by dust at the inner edge of the torus, and the large opacity of dust in that band couples the radiation so strongly to the torus matter that the radiation force is comparable to gravity (Pier & Krolik 1992a). When first proposed, this scheme was only an order of magnitude estimate because its authors did not attempt to find a self-consistent solution of both the infrared transfer problem and the force balance problem.

It is the object of this paper to show, via an idealized model, that self-consistent equilibrium solutions in which the torus is supported by infrared radiation force do exist. The model presented is admittedly highly simplified and rests on a number of rough approximations. However, it does contain all the zeroth-order physics of the problem, and, as will be shown, it is completely solvable analytically. Moreover, the solutions found demonstrate certain qualitative features that should apply to any more realistic description.

2. The Model

2.1. Qualitative presentation

Obscuring tori wrap around a central active nucleus. In their central “hole”, the matter must be largely transparent, so that viewers located along the axis can see the nucleus clearly (they then see a “type 1” AGN). On the other hand, on oblique and equatorial lines of sight, there is so much opacity to wavelengths from the near-infrared to soft X-rays that viewers in those directions see nothing but infrared radiation from the warm dust in the torus or very hard X-rays. The very fact that these tori are, indeed, “obscuring” means that they must act as light reprocessing machines which are heated from the inside and cooled from the outside. Radiation flux from the AGN passes through the torus (although suffering some drastic changes in spectrum *en route*), entering through its inner edge and departing through its upper and outer surfaces.

The key point behind the idea of supporting the geometric thickness of the torus by infrared radiation pressure is that the acceleration due to a given radiation flux \vec{F} is $\kappa\vec{F}/c$, where κ is the opacity per unit mass. The luminosity $L_{E,eff}$ capable of balancing the gravity of a mass M in spherical symmetry (the “effective Eddington luminosity”) is therefore $4\pi cGM/\kappa$, inversely proportional to the opacity. Because the opacity of dust per unit mass of gas is an order of magnitude greater than the Thomson opacity per unit mass when the radiation temperature is in the range 100–1000 K (Semenov et al. 2003), $L_{E,eff} \sim 0.1L_E$ for predominantly infrared light passing through dusty gas (this argument can be rephrased more precisely in terms of the divergence of the radiation pressure tensor, but its essential grounding still lies in the relatively high opacity of dusty gas). Enhanced heavy-element abundances likely lead to larger than local dust/gas ratios; where that is the case, $L_{E,eff}/L_E$ might be even smaller. Luminosities $\sim 0.1L_E$ are commonly expected in AGN, so if a significant part of the flux striking the inner surface of the torus can be converted to mid-IR wavelengths, radiation forces comparable to gravity can easily result.

Rotational support against gravity is so common in astrophysical contexts that it is entirely plausible to suppose that it is important here, too. However, the matter of the torus must have an effective collision rate at least as large as the orbital frequency. If it is fluid, this follows by definition. If it is highly clumped, this condition is compelled by the requirement that the torus be consistently opaque (Krolik & Begelman 1988). When the average line of sight through the torus has at least one clump on it, the mean collision rate of clumps is at least the orbital frequency. If these collisions are at all dissipative, one might expect the torus matter to settle into the plane normal to the total angular momentum and no longer be geometrically thick.

Adding radiation to the picture changes this conclusion. Radiation diffusing through the equatorial plane of a geometrically thin but optically thick annular structure quickly develops a large vertical flux in the region just outside its inner edge because that is the most direct path out of the opaque matter. At the order of magnitude level, this vertical flux is $\sim (H/r_{\text{in}})L/(\pi r_{\text{in}}^2)$, where the inner radius of the annulus is r_{in} and its half-thickness is H . The upward acceleration it creates, $(\kappa/c)(H/r_{\text{in}})L/(\pi r_{\text{in}}^2)$, competes with the downward acceleration of gravity, $(H/r_{\text{in}})(GM/r_{\text{in}}^2)$. Because the same factor of H/r_{in} enters the expressions for both the acceleration due to radiation and the acceleration due to gravity, if the magnitude of the flux is comparable to or greater than the effective Eddington flux, the annulus expands vertically. Greater thickness leads, of course, to interception of more light in a manner exactly balancing the growing magnitude of the vertical gravity.

A corollary of oblique flux producing a force comparable to gravity is that the radial component of the radiation force is also comparable to gravity. If this is so, radial force balance demands a rotation rate that is sub-Keplerian. Because the radial flux diminishes outward faster than $\propto r^{-2}$ as flux is diverted to the vertical direction, in equilibrium the specific angular momentum of the torus must increase outward, approaching Keplerian.

2.2. Self-consistent solution in the torus interior

In a real obscuring torus, the optical through soft X-ray continuum of the active nucleus is absorbed in a thin layer along its inner edge, where warm dust reprocesses the nuclear luminosity into the infrared. This inner edge is a complicated place, as we will discuss below. We therefore begin with the simpler problem of finding a self-consistent description of dynamics and radiation transfer in the torus interior. A more precise definition of the boundaries of this region, and therefore the domain of applicability of these results, will be given in the following subsection.

The simplest non-trivial geometry in which this picture can be explored is 2-d axisymmetry. Adopting cylindrical coordinates r and z , we write the equation of hydrostatic equilibrium for radiation and rotation balancing gravity as

$$\kappa \vec{\mathcal{F}}/c = -\vec{g}_{\text{eff}} = r\Omega^2(1 - j^2)\hat{r} + z\Omega^2\hat{z}, \quad (1)$$

where Ω is the local orbital frequency and the gas's specific angular momentum is $jr^2\Omega$. Note that we are supposing that gas pressure gradients are entirely negligible. We also adopt three simplifying assumptions, all appropriate to flattened geometries. First, we take Ω at all heights z to be the rotation rate of a circular orbit in the torus midplane at cylindrical radius r . Second, we follow only the component of angular momentum parallel to the torus

axis, and j is assumed to be a function of r alone. Third, we approximate the vertical component of the gravity by $z\Omega^2$. This last approximation would be exact if we evaluated Ω at the actual local value of z , rather than at $z = 0$.

Ideally, to find the flux, one would solve a complete transfer problem at all relevant frequencies for all photon directions. Here we take a much simpler approach: the gray diffusion approximation, using a thermally-averaged opacity. In this approximation, the flux is given by

$$\vec{\mathcal{F}} = -\frac{c}{3\kappa\rho}\nabla E, \quad (2)$$

where ρ is the gas density and E is the radiation energy density. Under the assumption of hydrostatic balance (eqn. 1), the radiation energy density and the dynamics are related by

$$-\frac{1}{3\rho}\nabla E = r\Omega^2(1-j^2)\hat{r} + z\Omega^2\hat{z}. \quad (3)$$

If the only source of infrared radiation is the conversion via dust reradiation of optical and ultraviolet photons at the inner edge of the torus, then in the body of the torus

$$\nabla \cdot \vec{\mathcal{F}} = 0. \quad (4)$$

It can also be of interest to explore the effect of distributed sources of infrared photons. These may be created, for example, by local heating due to Compton recoil when hard X-rays penetrate deep in the torus material (as discussed, e.g., in Chang et al. 2006) or by the absorption of locally-generated starlight. When there are distributed sources, the right-hand-side of equation 4 may be non-zero. For the purposes of this paper, however, we adopt the simple assumption of no internal sources. With that assumption, the diffusion equation becomes

$$\nabla \cdot \frac{c}{3\kappa\rho}\nabla E = 0. \quad (5)$$

Combining equation 5 with equation 3 gives

$$\nabla \cdot \left(\frac{c}{\kappa} \vec{g}_{\text{eff}} \right) = \nabla \cdot \left\{ \frac{c}{\kappa} [r\Omega^2(1-j^2)\hat{r} + z\Omega^2\hat{z}] \right\} = 0. \quad (6)$$

Detailed radiation transfer studies of obscuring tori consistently find that their interior temperatures are in the range 100–1000 K (Pier & Krolik 1992b, Efstathiou & Rowan-Robinson 1995, Granato et al. 1997, Nenkova et al. 2002). According to the most recent dust opacity models (e.g., Semenov et al. 2003), the Rosseland mean opacity for gas of Solar abundances and normal dust content is $\simeq 10$ – 30 times greater than Thomson and has no consistent trend within this temperature range, instead exhibiting only a few mild local

maxima and minima; the ratio of the largest opacity to the smallest is no more than ~ 3 . On this ground, we approximate κ as exactly constant. Equation 6 then reduces to

$$\frac{1}{r} \frac{\partial}{\partial r} [r^2 \Omega^2 (1 - j^2)] + \frac{\partial}{\partial z} [z \Omega^2] = 0. \quad (7)$$

Although the black hole mass may be larger than the stellar mass enclosed within the torus, it is easy to allow for potentials more general than a simple point-mass by writing $\partial \ln \Omega / \partial \ln r = -\alpha$. Then, for any particular potential described by $\Omega(r)$, equation 7 determines the unique $j(r)$ permitting a self-consistent solution. Written in terms of α , equation 7 becomes

$$r \frac{dj^2}{dr} + 2(1 - \alpha) j^2 = 3 - 2\alpha, \quad (8)$$

which has the solution

$$j^2(r) = [j_{\text{in}}^2 + f(\alpha)] \left(\frac{r}{r_{\text{in}}} \right)^{2(\alpha-1)} - f(\alpha), \quad (9)$$

where r_{in} is the radius at which the higher-energy photons are converted to infrared, $j_{\text{in}} = j(r_{\text{in}})$, and $f(\alpha) = 0.5(3 - 2\alpha)/(\alpha - 1)$. When $\alpha = 3/2$ (a point-mass potential), $f(\alpha) = 0$ and $j(r) = j_{\text{in}}(r/r_{\text{in}})^{1/2}$. When $\alpha = 1$ (a logarithmic potential), a logarithmic dependence replaces the power-law: $j^2(r) = j_{\text{in}}^2 + \ln(r/r_{\text{in}})$.

Assuming that the point where $j = 1$ marks the outer edge of the torus, we can use this solution to find the span of radii over which the torus exists. For $\alpha \neq 1$, it stretches from r_{in} to

$$r_{\text{max}} = r_{\text{in}} \left[\frac{1 + f(\alpha)}{j_{\text{in}}^2 + f(\alpha)} \right]^{1/[2(\alpha-1)]}; \quad (10)$$

in the special case of the logarithmic potential, $r_{\text{max}} = \exp(1 - j_{\text{in}}^2)$. As Figure 1 illustrates, for fixed j_{in} , the breadth of these tori stretches moderately as the slope of the potential steepens: for $j_{\text{in}} = 0.5$, r_{max} rises from $\simeq 2.1r_{\text{in}}$ for $\alpha = 1$ to $4r_{\text{in}}$ for $\alpha = 1.5$. Not surprisingly, r_{max} increases with diminishing j_{in} at fixed α .

With $j^2(r)$ known, equation 3 may be separated into two equations for ρ , which must be consistent with each other:

$$\rho = -\frac{1}{3z\Omega^2} \frac{\partial E}{\partial z} = -\frac{1}{3r\Omega^2 [1 - j^2(r)]} \frac{\partial E}{\partial r}. \quad (11)$$

It is instructive to rewrite in characteristic form the partial differential equation for E implied by the second equality:

$$\frac{dE}{ds} = \frac{\partial E}{\partial z} \frac{dz}{ds} + \frac{\partial E}{\partial r} \frac{dr}{ds} = 0, \quad (12)$$

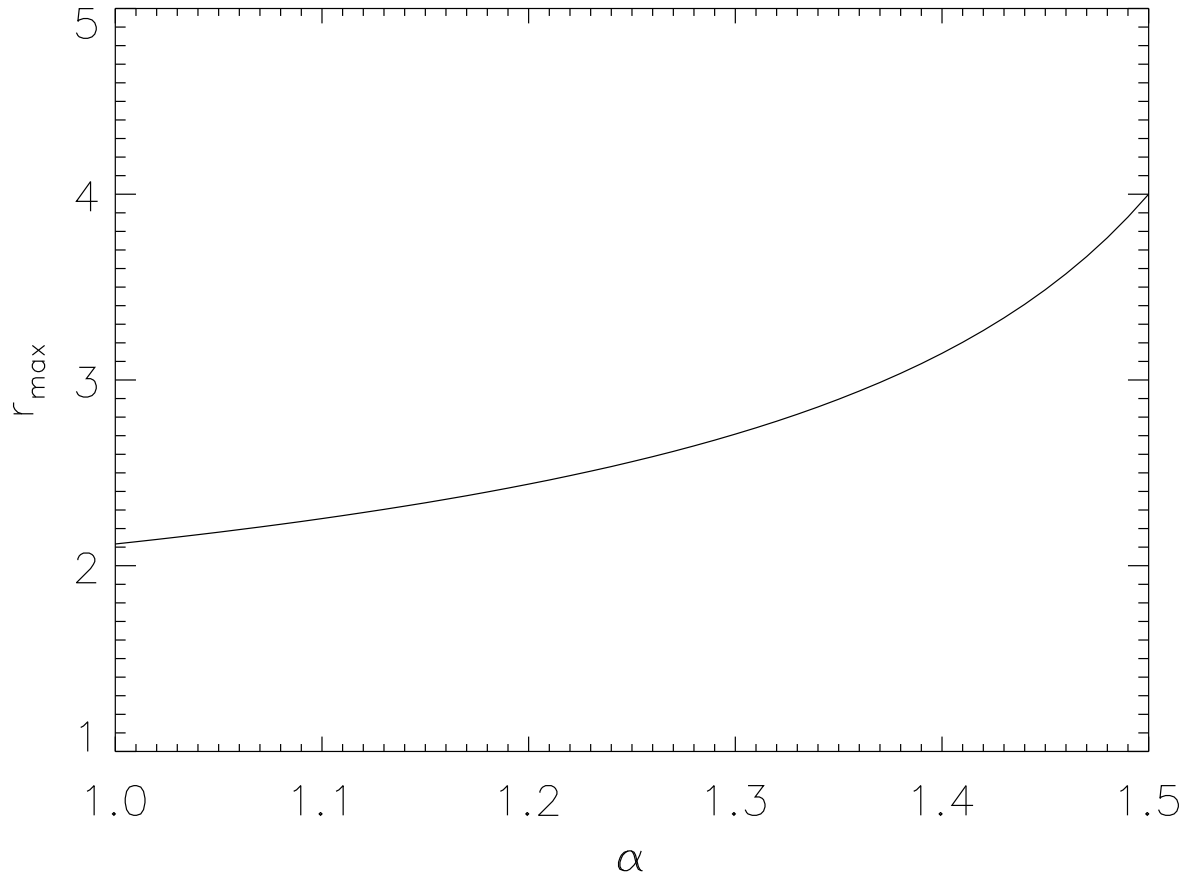


Fig. 1.— Maximum torus radius as a function of α for fixed j_{in} . The case illustrated is for $j_{\text{in}} = 0.5$.

with

$$\frac{dz}{ds} = \frac{1}{z} \quad \frac{dr}{ds} = -\frac{1}{r[1-j^2(r)]}. \quad (13)$$

From the characteristic form, we see that E is constant along contours parameterized by the pair of characteristic equations

$$\frac{1}{2}z^2 = s, \quad \int_{r_*}^r dr' r' [1 - j^2(r')] = -s + \lambda, \quad (14)$$

where r_* is arbitrary and we set the integration constant for $z(s)$ to zero by choosing $z = 0$ at $s = 0$. The radius at which a contour labelled by λ passes through $z = 0$ is given implicitly by the second characteristic equation. Equating the two expressions for s gives an explicit definition of the contours of constant E :

$$\frac{1}{2}z^2 + \int_{r_*}^r dr' r' [1 - j^2(r')] = \lambda. \quad (15)$$

Evaluating the integral, we find:

$$\frac{1}{2} \left(\frac{z}{r_{\text{in}}} \right)^2 + \frac{1}{4(\alpha - 1)} \left(\frac{r}{r_{\text{in}}} \right)^2 - \frac{1}{2\alpha} [j_{\text{in}}^2 + f(\alpha)] \left(\frac{r}{r_{\text{in}}} \right)^{2\alpha} = \lambda, \quad (16)$$

where we have redefined λ so as to absorb a number of terms that depend on the (arbitrary) r_* .

Because $j(r)$ depends only on $\Omega(r)$, the shapes of these contours depend only on the shape of the gravitational potential and on the boundary condition j_{in} . Generically, they are closed curves with principal axes parallel to the r and z axes, and elongated in the z direction. For example, when $\alpha = 3/2$, the contours are given by

$$\frac{1}{2} \left(\frac{z}{r_{\text{in}}} \right)^2 + \frac{1}{2} \left(\frac{r}{r_{\text{in}}} \right)^2 - \frac{1}{3} j_{\text{in}}^2 \left(\frac{r}{r_{\text{in}}} \right)^3 = \lambda. \quad (17)$$

That is, the larger j_{in} is, the more the contours stretch in the z direction.

We may solve an ordinary differential equation for $E(\lambda)$ along any path on which λ varies monotonically. For example, if we choose the path to run outward along the r axis from r_{in} , we have

$$\frac{dE}{d\lambda} = \frac{\partial E}{\partial r} \frac{dr}{d\lambda} = -3\rho\Omega^2. \quad (18)$$

In other words, knowledge of $\rho(\lambda)$ on this path is a prerequisite for accomplishing such a solution. Physically, this should come as no surprise: The run of radiation energy density

with position must certainly depend on how much matter there is with which to interact and how it is distributed. Somewhat arbitrarily, we choose to supply $\rho(r, z = 0)$ and integrate

$$\frac{dE}{dr} = -3\rho(r, 0)r\Omega^2 [1 - j^2(r)]. \quad (19)$$

It is convenient in this context (in which we have already written $\Omega \propto r^{-\alpha}$) to consider a density boundary condition that is also a power-law in radius: $\rho(r, 0) = \rho_{in}(r/r_{in})^{-\gamma}$. With this choice of $\rho(r, 0)$, every term on the right-hand-side of equation 19 is a power-law and the equation may be integrated exactly. The result is

$$E(r) = E_{in} - 3\rho_{in}r_{in}^2\Omega_{in}^2 \left\{ \frac{1 + f(\alpha)}{2 - 2\alpha - \gamma} \left[\left(\frac{r}{r_{in}} \right)^{2-2\alpha-\gamma} - 1 \right] + \frac{j_{in}^2 + f(\alpha)}{\gamma} \left[\left(\frac{r}{r_{in}} \right)^{-\gamma} - 1 \right] \right\}. \quad (20)$$

Note that if the power-law for $\rho(r, 0)$ were to extend to $r = \infty$, securing a finite optical depth would require $\gamma > 1$. However, because we cut off the power-law at a finite maximum radius, this restriction on γ is eliminated.

Once $E(r)$ in the equatorial plane has been found, one may directly determine E at *all* r and z by extending that solution into the plane following the characteristic curves that define its constant-value contours. The density ρ then follows from either of the equations 11.

2.3. Governing parameters, boundary conditions, and range of validity

So far we have identified three parameters that govern the character of these solutions: α , j_{in} , and γ . There are two more. One of these is $\tau_* \equiv \kappa\rho_{in}r_{in}$, which sets the optical depth scale. If the density declines outward, it must be at least several, or there will be nowhere where the diffusion approximation is valid. The other parameter is $Q \equiv 3\rho_{in}r_{in}^2\Omega_{in}^2(r_{in})/E(r_{in}, 0)$, whose physical meaning is most clearly seen when rewritten in terms of more familiar quantities:

$$Q = 3 \frac{\tau_*}{h} \frac{M(< r_{in})}{M_{BH}} \frac{\kappa_T}{\kappa} \frac{L_E}{L}, \quad (21)$$

where $M(< r_{in})$ is the total mass interior to r_{in} , and M_{BH} is the mass of the central black hole alone (which is what determines L_E in the usual definition). The factor h is the amount by which the optical depth of the torus enhances $E(r_{in}, 0)$ over the value it would have if the radiation could stream out freely. Because we expect the torus to be optically thick in the mid-infrared, but radiation can escape freely through the axial hole, $h \sim \tau_*/[1 + (\tau_* - 1)\phi]$, where ϕ is the fraction of solid angle that is open as viewed from the position $(r_{in}, 0)$. From

the statistics of type 1 versus type 2 AGN, we might suppose that $\phi \lesssim 1/2$. If $\tau_* \sim 10\text{--}30$, then $h \gtrsim 2$. Reasonable values of Q would then be $\sim 0.3\text{--}30$.

Our approximations do not hold at all locations, so it is important to mark off carefully the region of the r - z plane in which we can apply them. Because the phenomenology points us strongly toward a density distribution with an inner hole, we need to define an inner radial edge, within which the matter is optically thin. Unfortunately, we do not know the shape of this inner edge *a priori*; indeed, that shape is likely the result of some rather complicated dynamics, as will be discussed in the next several paragraphs. In this paper, whose goal is merely to demonstrate the possibility of thick structures supported by radiation pressure, we simply choose a vertical inner edge, i.e., $r_{\text{edge}}(z) = r_{\text{in}}$. Even if r_{edge} were a function of z , the solution we have derived in the previous subsection would still hold wherever $r > r_{\text{edge}}$. The extension of $E(r, 0)$ into the full r - z plane is entirely independent of the exterior boundary conditions because the hydrostatic balance condition substitutes, in effect, for boundary conditions in determining the interior diffusion solution. Reconciliation of our interior solution with the exterior boundary conditions will also be discussed later in this section. When we know more about $r_{\text{edge}}(z)$, that knowledge will change the size and shape of the region where our hydrostatic diffusion solution applies, but will not alter its nature in the torus interior.

Unfortunately, a proper determination of the position of the inner edge is far beyond the scope of this initial effort (Pier & Voit 1995 present a simplified model). Although the problem is superficially similar to the one treated here (simultaneously solving the equations of 2-d radiation transfer and 2-d hydrostatic equilibrium), several new effects become important at the edge and drastically complicate the problem. There is a large outward force from absorption and scattering of the optical/UV continuum arriving directly from the nucleus; there is also a comparably large, but inward, force due to the infrared flux emerging from the torus. Because the most important effects for both occur across photospheres (at different places for the different wavelengths, of course) the diffusion approximation is wholly inadequate for both. Gas pressure gradients, although (by assumption in this model) unimportant in the bulk of the torus, can also become significant locally.

In one respect, evaluating the force exerted by the optical/UV continuum is relatively simple: it has a single point-like source at the nucleus, so its transfer problem is essentially one-dimensional along radial rays (departures from true one-dimensionality arise only to the degree that the albedo of dust permits scattering to spread the beam). On the other hand, the opacity, far from being roughly constant, is a strong function of the radiation intensity, making this transfer problem highly nonlinear. At the inner edge of the torus, the gas can be photoionized and, in some cases, radiative heating can warm the dust above its sublimation

temperature. In addition, photoionization heating may raise the gas’s temperature high enough for it to destroy the dust by sputtering.

The only simple aspect of the infrared transfer problem is its qualitative behavior in two extreme geometric limits: In the limit of infinitesimal opening angle, the infrared intensity would be identically constant across the central hole; in the limit of very large opening angle, it would be considerably smaller along the axis than at the torus’s inner edge. However, because its principal opacity is also due to dust, many of the same difficulties that apply to the optical/UV continuum at the torus’s inner edge also apply to the infrared. In addition, because its sources are distributed, the solution is thoroughly 2-d and global. At the order of magnitude level, the infrared intensity in the central hole is likely to be comparable to or greater than the intensity of the optical/UV continuum precisely because of the blanketing provided by the optically thick torus; we have hidden this ratio in the $h(\tau_*)$ fudge factor already introduced. The total force it exerts on the gas in the inner edge region is determined by the contrast in intensity between the main body of the torus and the axis. In rough terms, we expect this fractional contrast to increase from the midplane upward because the fraction of “open sky” seen from a position on the axis increases upward, but to be quantitative about this dependences requires a proper 2-d global transfer solution.

Further complications can be caused by strong local gas pressure gradients, which are entirely absent in our model for the torus interior. Because the opacity of dust in the optical/UV is considerably greater than in the infrared, the radiation force due to this band is expressed across a much narrower zone than that due to the infrared. As an immediate consequence, sharp gas pressure gradients are likely to be created across these short lengthscales, even though the total gas pressure contrast from the torus body to the outside may not be that large. Gas pressure effects introduce further nonlinearity into the transfer problem because the gas’s equation of state is also strongly dependent on the radiation intensity.

Summarizing this qualitative discussion, we expect the location and shape of the inner edge to be the immediate result of balancing the opposing radiation and gas pressure gradient forces in the context of a rapidly changing physical state for the gas. Over longer timescales, mass flux balance will also come into play. As matter is ionized and heated at the extreme inner edge of the torus, it rushes away toward the lower pressures found at higher altitudes in the torus hole and beyond (Krolik & Begelman 1986, Balsara & Krolik 1993). To achieve a steady state, matter must accrete through the torus in order to replace the evaporated matter. The accretion rate is controlled by angular momentum transport; if, as is common in other disks, this is due to MHD turbulence, the problem is further complicated. Thus, determining the position of the inner edge is a much more difficult problem than solving for the static structure of the torus interior.

The outer radial edge is determined by the requirement that $j(r) \leq 1$; greater j would make hydrostatic equilibrium impossible. Although there is no automatic physical inconsistency created by placing the outer radial edge where $j < 1$, doing so begs the question of the dynamical state of the matter beyond: how does it make the transition from partial radiation force support to rotational support? The diffusion approximation is valid only within those regions whose optical depth to infinity is > 1 . Consequently, our solution should not be extended beyond the surface on which the vertical optical depth $\tau_z = \int_z^\infty dz' \kappa \rho(r, z') = 1$. Even if our approximations remained valid at small optical depth, one might define the torus edge as its infrared photospheric surface in any case.

At the photosphere we have another boundary condition, but one that can be applied only approximately: the flux as estimated by the diffusion approximation should roughly match the flux as estimated on the basis of free-streaming. Because we equate the diffusive flux with the flux necessary for hydrostatic balance, this condition amounts to requiring that

$$|\vec{g}_{\text{eff}}/\kappa| \sim E(r, z) \quad (22)$$

where $\tau_z = 1$. Unfortunately, the only way we can locate the photosphere is in terms of the density distribution derived from the diffusion equation. Outside the photosphere, this density distribution cannot be completely correct, yet what we mean by the location of the photosphere is the curve $z_{ph}(r)$ defined by $\int_{z_{ph}}^\infty dz \rho(r, z) \kappa = 1$. In other words, we find the photosphere using the density distribution in exactly that region where we know it least well. A further uncertainty is introduced by the fact that we can estimate to an accuracy of only a factor of ~ 3 the radiation energy density required to carry the flux in the optically thin regime. For all these reasons, we require equation 22 to be satisfied only to within a factor of 3.

There is also one additional constraint on acceptable solutions: if at anywhere along the radial axis $E < 0$, the solution is obviously unphysical. In practise, we find that the photospheric boundary condition is best matched at the smallest γ such that $E(r) > 0$ everywhere in the range $r_{\text{in}} \leq r \leq r_{\text{max}}$.

3. Results

With these thoughts in mind, consider the “typical” parameters $j_{\text{in}} = 0.5$, $\alpha = 1.5$, $\tau_* = 10$, and $Q = 3$. That is, rotational support is substantially depressed at the inner edge, the potential is that of a pure point-mass, the column density in the midplane is $\sim 10^{24} \text{ cm}^{-2}$, and $hL/L_E \simeq 1/3-1$. An acceptable solution requires $\gamma \simeq 0.5$, that is, the density declines slowly outward in the equatorial plane. If the matter density declines more steeply, there is

too little optical depth in the torus, and the energy density outside the photosphere predicted by the diffusion approximation is substantially larger than what is required to carry the flux in the optically thin regime; if the matter density declines more slowly, the optical depth is too great, forcing E to go negative. The successful solution that results from a compromise between these two extremes (i.e., $\gamma = 0.5$) is illustrated in Figure 2. Full Keplerian support is reached at $r_{\max} = 4r_{\text{in}}$. As expected, the contours of radiation energy density inside the torus are extended upward; this is exactly what one would expect when the radiation finds it easier to move vertically than radially. Note that, by assumption, the local temperature $T = (E/a)^{1/4}$, so the greatest temperature is found at $(r_{\text{in}}, 0)$, and it declines upward and outward from there. Contours of constant density, on the other hand, are extended radially. This, too, is entirely in line with expectations, given the difficulty of vertical support against gravity.

In both panels of Figure 2, a white curve shows the location of the photospheric surface on the top of the torus. Formally, our solution is invalid outside this white curve, as the diffusion approximation does not well describe the relation between energy density and flux in optically thin regions. Although much of the volume shown is in the optically thin region, most of its mass is within the optically thick portion of the torus. Consequently, while not taking too seriously the details of the solution in the optically thin zone, we can also be assured that they will not have serious impact on the issue of greatest concern here: the mass distribution within the torus.

Having located the outer boundaries within which this solution is physical, it is now time to consider its behavior on the inner boundary. As discussed earlier, we are not prepared to present a proper global infrared transfer solution that includes the central axial hole. Qualitatively, however, we might expect that the radiation intensity inside the torus hole would fall with height somewhat faster than $\propto (r_{\text{in}}^2 + z^2)^{-1}$ because the confinement due to the torus walls diminishes as its surface is neared. In fact, in our fiducial model, $(r_{\text{in}}^2 + z^2)E(r_{\text{in}}, z)/E(r_{\text{in}}, 0)$ falls slowly with increasing z , reaching $\simeq 0.6$ where the photosphere intersects the inner edge. This sort of behavior therefore appears to be at least loosely consistent with what one might guess about transfer solutions inside the torus hole.

The density profile in the equatorial plane is a strong function of Q when all other parameters are held fixed. Larger Q demands a steeper profile: as it changes over the factor of 10 from 0.6 to 3.0 to 6.0, the density power-law demanded rises from -2.58 to 0.50 to 3.05. In other words, the density must fall more steeply outward when L/L_E is smaller. When $\gamma < 1$, of course, the integrated optical depth is dominated by the outermost radius; solutions in this regime must involve very sharp cut-offs in the density profile at the outer radius.

Greater rotational support at the inner edge means that full Keplerian angular momentum is reached at a smaller radius. For example, if $j_{\text{in}} = 0.75$ but the other parameters are held fixed at their fiducial values, $r_{\text{max}} = 1.76r_{\text{in}}$, and the matter density must rise outward quite steeply ($\gamma = -4.71$) for there to be enough optical depth across this diminished radial thickness; otherwise, the boundary condition matching the diffusion approximation energy density and the free-streaming energy density cannot be satisfied. Conversely, if the fractional angular momentum support at the inner edge is much smaller, r_{max} is much larger and the density falls steeply outward: for $j_{\text{in}} = 0.25$, $r_{\text{max}} = 15.8r_{\text{in}}$ and $\gamma = 1.71$.

It is possible that distributed stellar mass may contribute significantly to the gravitational potential in the torus region. If so, orbital speeds will decline more slowly with increasing radius than in the Keplerian prediction. When this is the case, the equatorial density profile able to produce an equilibrium switches from one that gradually falls outward to one that gradually rises. For example, for $j_{\text{in}} = 0.5$ and $Q = 3$, γ drops from 0.5 to -0.19 as α falls from 1.5 to 1.1.

The optical depth parameter τ_* does not appear explicitly in the differential equations, so the shapes of the matter and energy density contours, as well as the γ required by the radiation energy density boundary condition at the photosphere, do not depend on it. However, the outline of the torus that results *does* change with τ_* because the photosphere (not surprisingly) rises higher and higher with increasing optical depth.

4. Consequences and Comparison with Observations

We have found that hydrostatic radiation-supported solutions can be found for plausible parameters, particularly when Q is within a factor of several of unity. For these solutions to be found in real AGN, two additional conditions must be satisfied: the matter’s angular momentum must be redistributed so that the equilibrium $j(r)$ is achieved; and the radial matter density profile in the equatorial plane must be adjusted to the right shape. It is possible that both may be achieved as a result of the magneto-rotational instability and the magnetic torques created by the MHD turbulence it drives. This is because j_{in} may be viewed as a function of γ : a matter density profile in the equatorial plane that does not fall as rapidly, or even rises outward (i.e., a smaller γ) is consistent with dynamical equilibrium when the fractional rotational support at the inner edge is greater.

Whether this actually happens in practise is uncertain. In conventional global disk simulations, MHD turbulence very efficiently redistributes angular momentum until it reaches a nearly-Keplerian radial profile (De Villiers et al. 2003). If that happened here, hydrostatic

balance would be possible only if accompanied by a substantial positive $\nabla \cdot \vec{\mathcal{F}}$. This might perhaps be supplied by local sources of heat, such as stars or Compton-heating due to hard X-rays that penetrate the bulk of the torus, but if sources such as these are inadequate, the disk would be forced to collapse to a thin configuration. On the other hand, in this context the equilibrium angular momentum distribution reached as a result of MHD turbulence might actually be the one required by this model (eqn. 9) because the net “gravity” has been effectively reduced by the outward radiation force.

In this context, it is notable that the velocity profile of the maser spots in NGC 1068 is $\propto r^{-0.3}$, rather than $\propto r^{-0.5}$ as one might expect from circular orbits in a point-mass potential (Greenhill et al. 2006). Our model predicts a rotational speed that always declines more slowly outward than simple circular orbits in the gravitational potential would dictate; for example, the mean rotational speed is constant as a function of radius when $\alpha = 1.5$. Thus, a shallow rotation curve may not signal a stellar contribution to the gravitational potential—it could instead be a symptom of radiation support.

Maser kinematics can also be used to estimate the central mass, either from the magnitude of the circular speeds or from the acceleration a seen in maser emission on the direct line of sight to the nucleus (although the circular speed is a more easily-observed quantity, a has been measured in four examples: Henkel et al. 2002 and references therein). In the former case, the mass inferred on the basis of Keplerian orbits is $v^2 r / G$, in the latter, ar^2 / G . The sub-Keplerian rotation that directly follows from the presence of radial radiation forces means that this inferred mass is an underestimate of the true mass by a factor j^2 in both cases. If the maser emission is driven by X-ray excitation (Neufeld et al. 1994), it takes place very close to r_{in} , so the relevant value of j is j_{in} .

Interestingly, the shape of the angular momentum profile required for equilibrium depends only on the underlying gravitational potential, and in this respect is a comparatively robust prediction of the model. On the other hand, because j_{in} is related to γ through the detailed equilibrium solution, which in turn depends on approximations like the photospheric boundary condition, their quantitative relationship is dependent on the quality of the several approximations made here.

We have also seen that a relatively small change in Q requires a large change in density profile: γ falls from $\simeq 3$ to $\simeq -2.5$ when Q falls from 6 to 0.6. If the optical depth is held fixed, Q is primarily dependent on L/L_E , to which it is inversely proportional. A consequence of this model, therefore, is that geometrically thick tori may be associated only with AGN having L/L_E within a range not much greater than a factor of 10, logarithmically centered on $L/L_E \sim 0.3$. Although the measurement of Eddington luminosity ratios is still very difficult, this range is easily consistent with the data in hand (e.g., the maser-based measurement of

the black hole mass in NGC 1068: Greenhill et al. 1996, Gallimore et al. 1996; the somewhat shakier black hole masses from reverberation-mapping: Metzroth et al. 2006 and references therein; or the still shakier inferences from photoionization-scaling: McLure & Dunlop 2004).

More precisely, if stellar contributions to the gravitational potential are negligible, the fact that $\kappa_T/\kappa \sim 0.03\text{--}0.1$ for warm dust implies that tori should be puffed up by radiation whenever $L/L_E \sim (0.03\text{--}0.1)\tau_*/h$. The ratio $\tau_*/h \sim 1 + (\tau_* - 1)\phi$, so it may vary over a modest range, from ~ 1 to a few, depending on the total optical depth through the torus and the shape of the inner hole. Infrared radiation pressure cannot provide predominantly vertical support against gravity unless the torus is optically thick in the mid-infrared; if it were optically thin, the flux would emerge more or less radially. When $\gamma > 1$, this requirement means that τ_* cannot be less than a few. However, when $\gamma < 1$, as is often the case, most of the optical depth is found near the outer edge of the torus, so the lower limit on τ_* can be smaller. At the low end of the permitted optical depth range, we would also expect h to be no more than a few. Larger optical depth cannot lead to much greater values of h , however, because the axial hole through the torus creates an escape channel. This is why, although solutions can be found for arbitrarily large values of τ_* , they are unrealistic unless somehow L/L_E can be $\gg 1$.

Measurements of the total optical depth in the equatorial plane of obscuring tori are difficult to come by. The column density of matter on the line of sight can be measured directly by soft X-ray absorption (or at least a lower bound placed when the Compton depth is greater than unity). However, in most cases, we do not have any direct evidence of the inclination angle of the torus to our line of sight; even if we did, it would be difficult to constrain directly the optical depth along the equatorial plane, in general a direction oblique to our line of sight.

On the other hand, we can measure the statistical distribution of column densities to obscured AGN and compare it to the predictions of this model, although this calculation is somewhat sensitive to the looseness in our location of the torus inner edge. The predicted probability of seeing a given column density is simply proportional to the solid angle associated with the polar angle producing that column. Typically, these solutions predict a wide range of associated column densities because lines of sight farther from the equatorial plane pass through densities exponentially lower than those closer to the plane. Because we are primarily interested in $\tau_* \sim 10$, which corresponds to $\tau_T \sim 0.3\text{--}1$, the range of expected Thomson depths is from $\sim 10^{-2}$ to $\gtrsim 1$, in good correspondence with observations (Risaliti et al. 1999, Treister et al. 2004). However, in contrast to the observational results, which tend to show a flatter distribution, there is a tendency for most of solid angle to be associated with the higher column densities. For example, if we take $\kappa_T/\kappa = 0.1$, in our fiducial

case the number of systems per logarithm of column density with $\tau_T \simeq 1$ is predicted to be $\sim 10\times$ the number seen with $\tau_T \simeq 0.01$ (Fig. 3). Qualitatively, the shape of this distribution has two sources: the solid angle per unit polar angle is, of course, greatest near the equatorial plane, where the densities are also greatest; and the high density region stretches away from the equatorial plane because the vertical component of gravity is relatively small there ($g_z \propto z$). Given the approximate character of our model, we expect that the prediction of a broad range of observed column densities should be fairly robust, but the exact shape of the predicted distribution is subject to significant uncertainty.

A different comparison with observations relates to the most fundamental reason why we believe the obscuration is geometrically thick: if the number of obscured AGN is comparable to or greater than the number of unobscured AGN having the same bolometric luminosity, then much of the sky surrounding the nucleus must be optically thick in the optical and ultraviolet. In principle, the solutions we have described also predict the fraction of solid angle obscured by the torus. For this question, however, the arbitrariness of our inner edge introduces an especially large systematic uncertainty. Because only small column densities are required to stop UV photons if there is a normal dust/gas ratio, any curvature of the inner edge could be significant. The following numbers should therefore be taken more in the way of examples than as serious predictions. Nonetheless, if we temporarily leave aside these considerations, we can still estimate the obscured solid angle by taking these models at face-value. If the wavelength of interest has an opacity 100κ (corresponding to $\lambda \simeq 4000(10\kappa_T/\kappa)$ Å: Draine & Lee 1984), 89% of solid angle is opaque in our fiducial model. This corresponds to a half-opening angle of 27° . Not surprisingly, larger Q (lower luminosity relative to Eddington) leads to a smaller obscured fraction, but only slightly smaller: $Q = 6$ (for all other parameters fixed) makes a torus that blocks 85% of the sky (32° half-opening angle).

In summary, we have constructed a simple, and entirely analytic, model of how infrared radiation pressure can, in principle, support obscuring tori around AGN. The model employs numerous approximations and simplifications that would undoubtedly be improved in a more complete and realistic picture. Most notably, a true transfer solution, rather than one adopting the diffusion approximation, would allow a proper connection to the boundary conditions at the photosphere of the obscuring matter. Frequency-dependent opacities would also improve its realism, although probably not as dramatically. In its treatment of the gas, a more realistic model might allow for clumping, both in regard to the opacity and to permit the introduction of supersonic random motions. However, we also wish to point out that, to the degree vertical support is provided by radiation pressure, the necessity of supersonic motions—and therefore clumping—is diminished.

This model also raises a number of questions. For example, as already discussed, the required angular momentum profile may or may not be achieved. It is also unclear whether this equilibrium is stable to a variety of perturbations—smooth motions in the gas, clumping in the gas, departures from the equilibrium angular momentum profile—to name a few possibilities. It is similarly uncertain whether the equilibrium, even if stable, can be reached from a wide range of initial conditions.

Despite these questions, the complete analytic solvability of this model means that we can learn from it a number of interesting qualitative facts about radiation forces in this context. Specifically, we have shown that a density distribution for the obscuration can be found in which *both* radiation diffusion and dynamics are in equilibrium. This distribution, as demanded by the phenomenology of AGN, can obscure a sizable solid angle for reasonable parameters. We have also found that in order for the equilibrium to be possible, several conditions must be met: the luminosity of the nucleus must be within a factor of several of $0.1L_E$; because there is always a significant radial radiation force, the matter in the torus must orbit more slowly than in a Keplerian orbit; the Thomson depth of matter in the equatorial plane must be not too far from $\sim O(1)$; and the level of rotational support relative to Keplerian is linked to the radial profile of matter density in the equatorial plane, L/L_E , and the total optical depth of the matter.

I would like to thank Eliot Quataert, Norm Murray, Phil Chang, Todd Thompson, and Lincoln Greenhill for very stimulating conversations and several very helpful suggestions. I am also indebted to Eliot Quataert and Omer Blaes for a careful reading of the manuscript, and to the second referee, Mitch Begelman, for a thoughtful review. This work was partially supported by NSF Grant AST-0507455 and NASA Grant NNG06GI68G.

REFERENCES

- Antonucci, R.R.J. 1993, ARAA, 31, 473
- Balsara, D.S. & Krolik, J.H. 1993, Ap J, 402, 109
- Barthel, P. 1989, ApJ, 336, 606
- Beckert, T. & Duschl, W. 2004, A&A 426, 445
- Capetti, A., Macchetto, F.D. & Lattanzi, M.G. 1997, ApJ Letts, 476, L71
- Chang, P., Quataert, E. & Murray, N. 2006, in preparation

- De Villiers, J.-P., Hawley, J.F. & Krolik, J.H. 2003, *ApJ*, 599, 1238
- di Serego Alighieri, S., Cimatti, A., & Fosbury, R.A.E. 1994, *ApJ*, 431, 123
- Draine, B.T. & Lee, H.M. 1984, *ApJ*, 285, 89
- Efstathiou, A. & Rowan-Robinson, M. 1995, *MNRAS*, 273, 649
- Gallimore, J.F., Baum, S.A., O’Dea, C.P., Brinks, E. & Pedlar, A. 1996, *ApJ*, 462, 740
- Granato, G.L., Danese, L. & Franceschini, A. 1997, *ApJ*, 486, 147
- Greenhill, L.J., Gwinn, C.R., Antonucci, R.R.J. & Barvainis, R. 1996, *ApJLetts*, 472, L21
- Hao, L. et al. 2005, *AJ*, 129, 1795
- Henkel, C., Braatz, J.A., Greenhill, L.J. & Wilson, A.S. 2002, *A & A* 394, L23
- Jaffe, W. et al. 2004, *Nature*, 429, 47
- Kishimoto, M. 1999, *ApJ*, 518, 676
- Königl, A. & Kartje, J.F. 1994, *ApJ*, 434, 446
- Krolik, J.H., & Begelman, M.C. 1986, *ApJ Letts*, 308, L55
- Krolik, J.H., & Begelman, M.C. 1988, *ApJ*, 329, 702
- Lovelace, R.V.E., Romanova, M. & Biermann, P.L. 1998, *A&A*, 338, 856
- McLure, R.J. & Dunlop, J.S. 2004, *MNRAS*, 352, 1390
- Metzroth, K.G., Onken, C.A. & Peterson, B.M. 2006, *ApJ*, 647, 901
- Nenkova, M., Ivezić, Ž. & Elitzur, M. 2002, *ApJLetts*, 570, L9
- Neufeld, D.A., Maloney, P.R, & Conger, S. 1994, *ApJ Letts*. 436, L127
- Pier, E.A. & Krolik, J.H. 1992, *ApJLetts* 399, L23
- Pier, E.A. & Krolik, J.H. 1992, *ApJ*, 401, 99
- Pier, E.A. & Voit, G.M. 1995, *ApJ*, 450, 628
- Risaliti, G., Maiolino, R. & Salvati, M. 1999, *ApJ*, 522, 157

Sanders, D.B., Phinney, E.S., Neugebauer, G., Soifer, B.T. & Matthews, K. 1989, ApJ, 347, 29

Semenov, D., Henning, T., Helling, C., Ilgner, M. & Sedlmayr, E. 2003, A&A, 410, 611

Thompson, T., Quataert, E. & Murray, N. 2005, ApJ, 630, 167

Treister, E. et al. 2004, ApJ, 616, 123

Zakamska, N. et al. 2005, AJ, 129, 1212

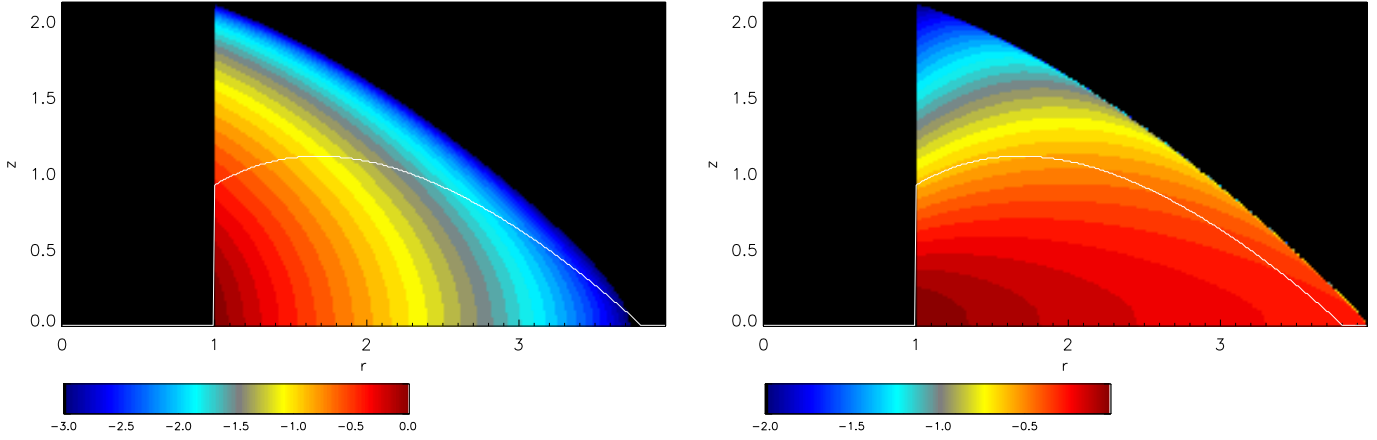


Fig. 2.— A solution with $j_{\text{in}} = 0.5$, $\alpha = 1.5$, $\gamma = 0.5$, $\tau_* = 10$, and $Q = 3$. Left panel: Radiation energy density. Right panel: Matter density. In both, the scale is logarithmic, and the white curve shows the surface on which $\tau_z = 1$, the photosphere on the top of the torus.

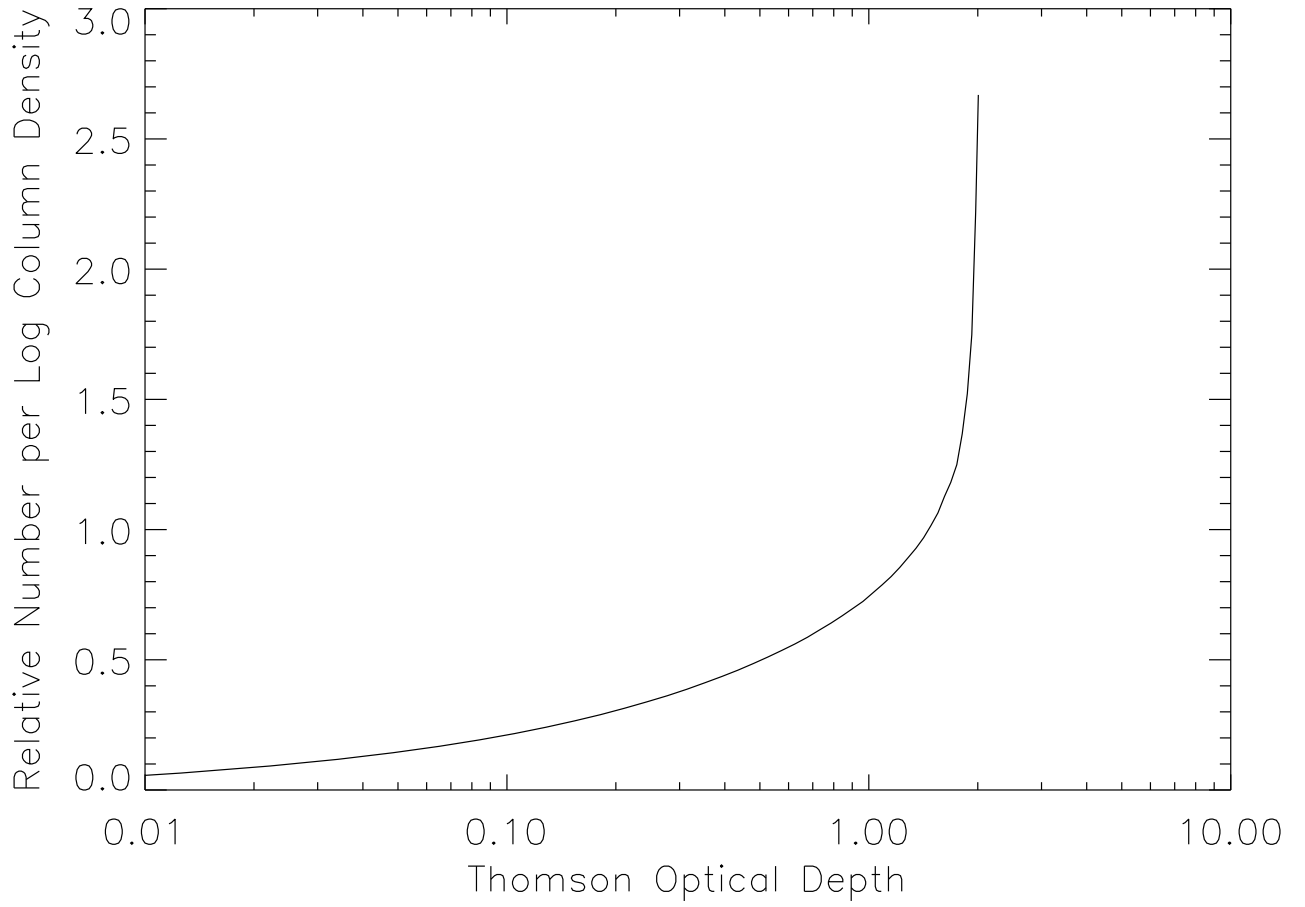


Fig. 3.— The predicted column density distribution for the solution with the same parameters as Fig. 2.